A detailed chemical kinetic modeling and experimental investigation of the low and high temperature chemistry of n-butylcyclohexane

Short running title (less than 40 characters): n-Butylcyclohexane: experiments & model

William J. Pitz[1], Jinhu Liang[2,3], Goutham Kukkadapu[1], Kuiwen Zhang[1,1], Christine Conroy[2], John Bugler[2], Henry J. Curran[2]

[1]Materials Science Division, Lawrence Livermore National Laboratory, P. O. Box 808, Livermore, CA94551 USA

[2]Combustion Chemistry Centre, School of Chemistry, Ryan Institute, MaREI, National University of Ireland Galway, Galway, Ireland

[3]School of Environmental and Safety Engineering, North University of China, Taiyuan, 030051, China

Acknowledgements

The work at LLNL was supported by the U.S. Department of Energy, Vehicle Technologies Office (program managers Mike Weismiller and Gurpreet Singh) and performed under the auspices of the U.S. Department of Energy by Lawrence Livermore National Laboratory under Contract DE-AC52-07NA27344. NUIG acknowledges the financial support of Saudi Aramco, the Irish Research Council and Science Foundation Ireland under grant numbers 15/IA/3177 and 16/SP/3829. Jinhu Liang acknowledges the International Scientific Cooperation Projects of Key R＆D Programs in Shanxi Province via project number 201803D421101.

Abstract

Chemical kinetic models of gasoline, jet, and diesel fuels and their mixtures with bio-derived fuels are needed to assess fuel property effects on efficiency, emissions, and other performance metrics in internal combustion and gas turbine engines. Since these real fuels have too many fuel components to be included in a chemical kinetic model, surrogate fuels containing fewer

[1] Present address: Convergent Science Inc., 6400 Enterprise Ln, Madison, WI 53719, USA

components are used to represent them. These surrogate fuels mimic chemical classes or molecular structures contained in the real fuel. One of the important chemical classes in gasoline, jet, and diesel fuels comprises cyclohexanes. Cyclohexanes comprise about 30% or more by weight in diesel fuel. Also, Mueller et al. 2012 proposed n-butylcyclohexane as a component in a 9-component surrogate palette to represent the ignition properties, distillation curve, density, and molecular structures of a diesel certification fuel. In this work, experimental measurements of the ignition delay times of n-butylcyclohexane in a shock tube and in a rapid compression machine are reported over a wide range of temperature, pressure and equivalence ratio important for enabling the validation of a chemical kinetic model for n-butylcyclohexane for combustion in diesel engines. The range of conditions are temperatures of 630–1420 K, pressures of 10, 30 and 50 bar, and equivalence ratios of 0.3, 0.5, 1.0 and 2.0 in ‘air’. A detailed chemical model is developed for n-butylcyclohexane to simulate its ignition at both low and high temperature conditions and at relevant elevated pressures. The experimentally measured ignition delay times are used to improve and validate the chemical kinetic model.

Keywords: *n-butylcyclohexane, shock tube, rapid compression machine, autoignition, chemical kinetic model*

1. Introduction

Cycloalkanes are an important class of compounds in transportation fuels. They have important properties for gas turbine applications where bicyclic cycloalkanes absorb significant quantities of heat to cool aircraft[1]. For oil-sand derived fuels, they are in much higher concentrations than present in conventionally-derived fossil fuels[2]. The combustion properties of cycloalkanes are unique. Their low temperature behavior falls between that of n-alkanes and olefins. They often show more negative-temperature-coefficient (NTC) behavior than olefins, but less than that for n-alkanes. When present in gasoline or diesel fuels, they affect the ignition properties in a subtle way. At lower temperatures, cycloalkanes form fuel radicals that react with O_2 to form olefins. This leads to the production of allylic radicals which are known to suppress ignition chemistry[3]. Since cycloalkanes are prevalent in gasoline, jet, and diesel fuels, these allylic radicals will suppress autoignition reactions particularly at intermediate temperatures (~ 800 K). Proper simulation of this suppression is essential for predicting the autoignition behavior of real fuels. The sooting behavior of cycloalkanes also has an important impact on soot emissions from combustion devices. Based on yield sooting index (YSI) measurements, the sooting tendencies of 2-ring cycloalkanes (e.g. decalin, YSI = 105) is significantly higher than that of n-alkanes (e.g. n-dodecane, YSI = 72) [4]. Although the aromatic content mainly controls the sooting behavior of real fuels, proper accounting of the sooting behavior of cycloalkanes may be necessary to accurately predict sooting behavior for real fuels.

Diesel fuel is a complex mixture and many surrogate components are needed in a diesel surrogate fuel to match the density, carbon/hydrogen ratio, distillation curve and ignition behavior of a target diesel fuel. When an optimization code is used to select diesel surrogate components[5], n-butylcyclohexane (nBCH) is often selected in significant concentrations

because it is helpful in attaining a match for these diesel properties. nBCH is present in two of the four surrogates developed to represent the properties of real diesel fuel (#2 diesel certification fuel) [6] and is at a level of 19% molar in the most high-fidelity surrogate (V2) for diesel. The development of a validated chemical kinetic model for nBCH is needed to complete a diesel surrogate fuel model to represent these diesel surrogates. This paper focuses on the auto-ignition behavior of nBCH because autoignition is one of the key properties controlling ignition phasing in diesel engines.

In previous experimental work on nBCH, Mao et al.[7] investigated the ignition behavior of nBCH in a shock tube (ST) and in a rapid compression machine (RCM) over a wide range of temperature, pressure and equivalence ratio. In a subsequent paper, Mao et al.[8] made additional RCM measurements at highly diluted conditions and at 10, 15 and 20 bar. They also made species concentration measurements in a flow reactor at 1 atm over a range of temperatures from 650 to 1075K, and equivalence ratios of 1 and 1.5. Natelson et al.[9] also studied nBCH oxidation in a flow reactor from 600 to 820 K at 0.8 MPa pressure, 120 ms residence time, at an equivalence ratio (φ) of 0.38 to determine its low temperature behavior. They measured species concentrations and observed NTC behavior from 670 to 825 K. Hong et al.[10] measured the shock tube ignition of nBCH and the time evolution of ȮH and water over a temperature range of 1280 to 1480 K, at pressures of 1.5 and 3 atm, for φ = 0.5 and 1.0. They found that nBCH had similar ignition delay times (IDTs) to cyclohexane, but shorter IDTs than methylcyclohexane. They also measured concentration histories of ȮH radicals and water at early times. They found that JetSurf version 1.1 [11] was not able to accurately reproduce the ȮH time histories.

A detailed chemical kinetic model for nBCH has been previously developed for high temperatures with a simplified model describing low temperature oxidation[12]. This model

(JetSurF2.0) has been used to successfully simulate premixed laminar flame speeds, species histories in a shock tube, and ignition behavior in a shock tube and a counter-flow flame. However, the model was limited in its ability to predict low temperature behavior. Natelson et al.[9] expanded the low temperature model in JetSurf1.1 [11] with a reaction scheme of 42 species and 80 reactions. It reasonably predicted the low temperature oxidation of nBCH in their flow reactor experiments. Mao et al.[7] tuned the Natelson et al. model with some modification to simulate their combined ST and RCM ignition data. In a subsequent paper, Mao et al.[8] proposed a detailed chemical kinetic model for the low and high temperature oxidation of nBCH. The chemical kinetic model was validated using experimental data from shock tubes, an RCM, a jet stirred reactor, and a flow reactor and the comparisons showed good agreement.

To aid in the development of improved mechanisms of nBCH, electronic structure calculations have been carried out by Ali et al.[13]. They computed more accurate fuel ring-opening rate constants by using a single-reference method (quantum composite G3B3). Seven channels for ring-opening were computed. The question of whether single-reference methods are sufficient or whether multi-reference methods are needed for these ring opening reactions remains to be resolved. In prior work on cyclohexane, a multi-reference method (CASPT2/cc-pVDZ) [14] was used to compute the fuel-ring opening reaction of cyclohexane directly to 1-hexene.

In this paper, new experiments are reported on the auto-ignition properties of nBCH in a shock tube and RCM that cover the full range of low and high temperature chemistry. Also, these experiments extend the pressure range previously studied in the literature to higher pressures. The upper limits of pressure are extended from 20 to 50 bar in the ST, and from 20 to 30 bar in the RCM. Since nBCH is a surrogate compound for surrogate mixtures to represent diesel fuel,

obtaining these higher pressures is important for applications in diesel combustion where typical pressures at ignition can be ~ 80 bar [15]. Also, developed herein is one of first chemical models for nBCH that covers both high and low temperature chemistry. It is validated using the new experimental data that covers higher pressures than previously attainable which is important for properly simulating diesel combustion.

2. Methods/Experimental

2.1 Shock tubes

Intermediate-pressure and high-pressure STs were utilized in this study to acquire IDTs. Experimental data at reflected shock pressures of 10 and 30 bar were obtained in the intermediate-pressure ST[16] and at 50 bar were obtained in the high-pressure ST[17]. Brief descriptions of both tubes will be given here with greater detail in [16, 17].

The intermediate-pressure shock tube consisting of a stainless-steel tube of 8.76 m in length, with an internal diameter of 6.35 cm. A double-diaphragm section divides the shock tube into a 3 m long driver section and a 5.73 m driven section. Polyethylene terephthalate films (KATCO) were used as diaphragms in all experiments. The driver gas used was helium (99.99% pure; BOC). The diagnostic system involves four pressure transducers, where the velocity of the incident shock wave was measured at three locations separated by known distances with the shock velocity extrapolated to the endwall. The incident shock velocity at the endwall was used to calculate the temperature and pressure of the mixtures behind the reflected shock wave using the equilibrium program Gaseq[18]. The pressure at the endwall was monitored using a pressure transducer (PCB; 113A24). The IDT is defined as the interval between the rise in pressure due to the arrival of the shock wave at the endwall and the maximum rate of rise of the pressure signal.

The high-pressure ST at NUI Galway (NUIG) has the same dimensions as the intermediate pressure tube. Aluminum plates were used as the diaphragm material, where the thickness of the diaphragms was chosen depending on the desired final shock pressure and varied from 0.8–2.0 mm. Six pressure transducers on the sidewall (PCB; 113A24) were used to measure the velocity of the incident shock wave, which was used to calculate the temperature of the mixtures behind the reflected shock wave using the program Gaseq[18]. Pressures behind the reflective shock wave were measured using the pressure transducer in the endwall (Kistler; 603B). The definition of IDT is the same as intermediate-pressure experiments. The pressure rise before ignition is approximately 3%/ms in the present shock tube. Estimated uncertainty limits of the measurements in both STs are ±15 K in reflected shock temperature, T_5, ±15% in IDT, τ, and ±1% in mixture concentration. The nBCH ST data are included as Supplementary Information.

2.2 Rapid compression machine

A heated twin-opposed piston RCM at NUI Galway [19-21] was used to the measure IDTs for nBCH/"air" mixtures at equivalence ratios of 0.5, 1.0 and 2.0, at pressures of 10 and 30 bar in the low to intermediate temperature range (630–975 K). The "air" used here is a mixture of O_2 and N_2/Ar/CO_2 in the molar ratio of 21/79. A brief description will be given here with details in[21, 22].

The twin-opposed pistons have creviced heads that can achieve a more homogeneous post-compression temperature compared to flat piston heads[23]. Compression times of approximately 16 ms are achieved with a compression ratio of approximately 9.0. Different desired compressed-gas temperatures and pressures are achieved by changing the initial temperature, pressure and inert gas composition (Ar/N_2 and N_2/CO_2). The mixing tank, manifold, reaction chamber and the two sleeve sections are heated using heating tapes, and the

temperatures are controlled by thermostats and thermocouples. Homogeneous mixtures of reactants were prepared manometrically inside a stainless-steel mixing tank according to the partial pressure of each component. For the ST and RCM experiments, n-BCH (purity 99%) was supplied by TCI. Oxygen (purity 99.99%), nitrogen (purity 99.95%), argon (purity > 99.5%), carbon dioxide (purity 99.95%) and helium (purity 99.99%) gases were supplied by BOC. All reagents were used without further purification. In order to avoid condensation, nBCH was injected via an injection port on top of the heated mixing tank at 393 K. A Kistler 6045B piezoelectric pressure transducer was used to obtain the pressure traces. Two-stage ignition phenomena were recorded for some experimental conditions. The IDT is defined as the time interval between the first local maximum pressure at end of compression to the maximum rate of the pressure trace rise due to ignition. Figure 1 is a typical pressure trace for nBCH oxidation, τ_{1st} is the first stage ignition delay time and τ_{total} is the total IDT. Both of the reactive pressure traces 1 and 2 show good repeatability of our experimental results from two similar experiments. To simulate facility effects including compression and heat losses, non-reactive pressure-histories were recorded in which oxygen was replaced by nitrogen in the mixtures which are converted to volume histories to be used in chemical kinetic simulations. Details of the experimental procedures are provided in [21, 22]. Uncertainties in compressed temperature and IDTs are

estimated to be less than 15 K and 5% [24], respectively. The nBCH RCM data, and the nonreactive volume histories are included as Supplemental Information.

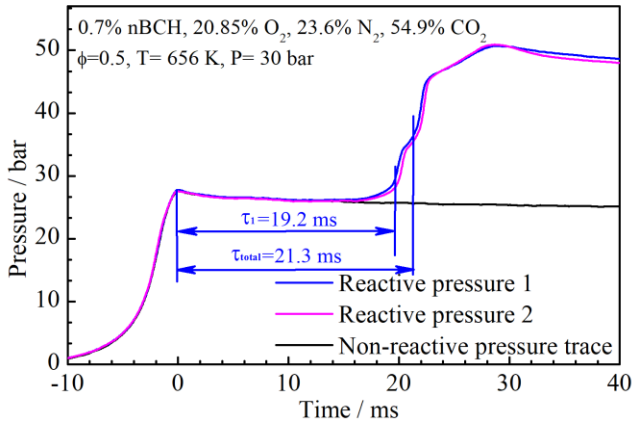

Figure 1. A typical pressure trace for nBCH oxidation in the NUIG RCM.

3. Model development

The nBCH model was constructed hierarchically starting with the C_0–C_4 base chemistry from AramcoMech2.0 [25]. The previously developed methylcyclohexane model[26] was added which has updates on its low temperature chemistry and includes a cyclohexane sub-model. Next, the nBCH model developed herein was added using analogous reaction rates from the updated methylcyclohexane model[26].

For the high temperature chemistry, the reaction classes below are included:

High Temperature Reaction Classes

1. Unimolecular fuel decomposition
2. H-atom abstraction from the fuel
3. Alkyl radical decomposition
4. Alkyl radical isomerization
5. H-atom abstraction reactions from alkenes
6. Addition of radical species O and OH to alkenes
7. Reactions of alkenyl radicals with HO_2, CH_3O_2, and $C_2H_5O_2$
8. Alkenyl radical decomposition

9. Alkene decomposition
10. Retroene decomposition reaction

For Reaction Class 1, rates of unimolecular fuel decompositions were adopted from Ali et al.[13]. For H-atom abstraction from the fuel (Reaction Class 2), rate constants for abstraction by ȮH on the nBCH ring were taken by analogy from theoretical rate constant fits for methylcyclohexane from Sivaramakrishnan et al.[27]. For other H-abstraction rate constants for the fuel, no rate constants were available and the acyclic reaction-rate rules from Sarathy et al.[28] are used. These acyclic rates are within 20% of cyclic rates that have been measured for the CH_2 groups on the MCH ring[27]. For alkyl radical decompositions (Reaction Class 3), rate constants from JetSurf 2.0 are adopted[12]. These rate constants are pressure-dependent, 9-parameter (Troe) fits. Based on the notes in JetSurf 2.0, these rate constants are based on acyclic rate constants from published work and from work-in-progress of Tsang and coworkers, e.g.[29]. For alkyl radical isomerization (Reaction Class 4), the rate constants used were generally estimated by Sirjean and Wang for NBCH as in JetSurf 2.0. For the isomerizations on the alkyl group only, the rates are from Sarathy et al.[28]. Concerning the chemistry of the cyclic alkenes formed from nBCH, all the n-butylcyclohexene isomers are included. To reduce the size and complexity of the model, the cyclic alkenyl radicals produced are lumped into the resonantly-stabilized form because these are the most likely to be formed. For addition of ȮH to alkenes (Reaction Class 6), the Waddington mechanism[30] is included for the cyclic alkenes because these reactions can be important in enhancing ȮH production. For other high temperature reaction classes, the reader is referred to the well-annotated mechanism for the source of the reaction rate expressions.

For the low temperature chemistry, the following reaction classes were included:

Low Temperature Reaction Classes

11. Addition of O_2 to alkyl radicals ($R + O_2 = ROO$)

12. R + ROO = RO + RO
13. R + HO_2 = RO + OH
14. R + CH_3O_2 = RO + CH_3O
15. Alkyl peroxy radical isomerization (ROO = QOOH)
16. Concerted eliminations (ROO = alkene + HO_2)
17. ROO + HO_2 = ROOH + OH
18. ROO + H_2O_2 = ROOH + HO_2
19. ROO + CH_3O2 = RO + CH_3O + O_2
20. ROO + ROO = RO + RO + O_2
21. ROOH = RO + OH
22. RO decomposition
23. QOOH = cyclic ether + OH (cyclic ether formation via cyclisation of diradical)
24. QOOH = alkene + HO_2 (radical site beta to OOH group)
25. QOOH = alkene + carbonyl + OH (radical site gamma to OOH group)
26. Addition of O_2 to QOOH (QOOH + O_2 = OOQOOH)
27. Isomerization of OOQOOH and formation of carbonylhydroperoxide and OH
28. Decomposition of carbonylhydroperoxide to form oxygenated radical species and OH
29. Cyclic ether reactions with OH and HO_2
30. Decomposition of large carbonyl species and carbonyl radicals

For Reaction Class 11, the rate of addition of nBCH radicals to O_2 was taken from Fernandes et al.[31] for cyclohexane and is used for nBCH radical sites on the ring. For radical sites on the alkyl group, acyclic rate constants from Miyoshi[32] are used following Bugler et al.[33]. Bugler et al. found these acyclic rate constants work well for C_5 and C_6 n-alkanes and iso-alkanes when comparing simulations to experiments of low-temperature ignition in RCMs and shock tubes. Similarly for the nBCH alkylperoxy ($R\dot{O}_2$) isomerization (Reaction Class 15), rate constants for isomerizations on the ring are taken from Fernandes et al.[31] and for isomerization on the alkyl group are taken from the recommendations of Bugler et al. who used *ab inito* rates from Sharma et al.[34]. For $R\dot{O}_2$ isomerizations between sites on the ring and on the alkyl group, *ab initio* rate constants for acyclic alkanes from Sharma et al. are used so that ring-strains in the transition states (TST) are assumed to be the same as in an acyclic alkane (except for the specific case mentioned below). The A-factors were adjusted for the reduction in the number of rotors lost in the TST compared to the acyclic alkane case. Originally, semi-empirically based rate constants for acyclic

alkanes from Sarathy et al.[28] were used for $R\dot{O}_2$ isomerizations between sites on the ring and on the alkyl group, but this resulted in ignition delay times that were too slow compared to experiments in the ST and RCM. For $R\dot{O}_2$ isomerization between the 2-site on the ring and the A-site on the alkyl chain (see Fig. 2 for carbon-site definitions in nBCH), the *ab initio* calculated rate from Weber et al.[26] for methylcyclohexane (MCH) was used. An activation energy reduction of ~ 3 kcal was made for an H-abstraction on a secondary site in nBCH compared to a primary site in MCH, and the A-factor was adjusted for reaction degeneracy. The A-factor was then multiplied by a factor of 2 to obtain better agreement with the measured ignition delays. For addition of hydroperoxyalkyl ($\dot{Q}OOH$) radicals radical to O_2 (Reaction Class 26), the rates for $\dot{R} + O_2$ were adapted from Miyoshi[32] and the pre-exponential factors were multiplied by 0.55 following Bugler et al. to obtain better agreement with the experimental validation set. For peroxy hydroperoxyl alkyl ($\dot{O}_2QOOH$) isomerization (Reaction Class 27), the rate constants were analogous to the isomerization of $R\dot{O}_2$ with some adjustments for axial and equilateral effects as noted in the mechanism file. For the rate constant selection of the other reaction classes, the reader is directed to the well-annotated mechanism.

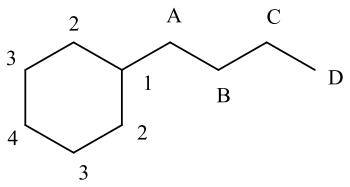

Figure 2. Labeling of nBCH carbon sites.

The rate constants in the mechanism were analyzed by Mech Checker tool (https://combustiontools.llnl.gov)[35] that identifies reaction rate constants which exceed theoretical limits, such as collision limits for bimolecular reactions and plausible limits for

unimolecular reactions over the temperature range encountered in combustion. The reaction rates that exceeded these limits were identified and corrected. One example of a reaction that had an issue was the addition of methyl radical to 2,5-cyclohexadienone at the site of the ketone carbon. The reverse of this reaction is a decomposition of an unsaturated, cyclic, alkoxy radical in the methylcyclohexane sub-mechanism which is part of the nBCH mechanism. The reverse rate of this reaction is a unimolecular decomposition reaction and was flagged by Mech Checker to have a maximum decomposition rate of 10^{17} s^{-1}. Unimolecular decomposition reaction rates are flagged if the rate exceeds 6×10^{12} s^{-1} at 300 K to 6×10^{13} s^{-1} at 3000 K based on unimolecular transition state theory. This reverse rate constant is about 8 orders of magnitude too high compared to known decomposition rates of alkoxy radicals. The reaction was fixed by specifying the rate constant in the reverse direction which is a unimolecular decomposition of alkoxy-type radical. The rate constant was specified by analogy t-butyloxy decomposition from Table 8 of Curran[36] as stated in the nBCH mechanism file.

The thermodynamic parameters for the species are very important because they are used to determine reverse rate constants. The C_1–C_4 species thermodynamic parameters were taken from Metcalfe et al.[37]. The THERM software[38] was used to compute the thermochemical properties of nBCH-related species. Group values were taken from Bozzelli[39]. Mech Checker was used to identify discontinuities in the thermodynamic fits and correct them. The mechanism is available as Supplemental Material.

4. Results and Discussion

The IDT results of the shock tube experiments and simulations are shown in Fig. 3 for equivalence ratios of 0.3, 0.5, 1.0 and 2.0 in ‘air’, temperatures from 670 to 1350 K and pressures of 10, 30 and 50 bar. For the 10 bar case, experimental data were limited to higher temperatures

(> 950K), except for the highest equivalence ratio, due to the interaction of the reflected shock wave with the contact surface which sends a compression wave back to the test location and results in the termination of the test time for ignition delay times exceeding ~2 ms[40]. The symbols represent the experimental data and the curves the simulations. The shock tube simulations were performed assuming constant volume combustion. The experimental results show that nBCH has NTC behavior in the low temperature region for pressures of 30 and 50 bar at equivalence ratios (ϕ) of 0.5, 1.0, and 2.0. At ϕ = 0.3, a nearly zero slope in the NTC region seen. Computed results show nearly the same behavior. Both the experimental and computed results show that the influence of pressure increases with equivalence ratio and more pressure effect is observed at lower temperatures (700–900 K). The simulated IDTs are most affected by a change in pressure from 10 to 30 bar at the temperature region below 1000K. The effect of ϕ is most evident when it increases from 0.5 to 1 for the 30 and 50 bar cases.

Simulations of chemical kinetic model were also compared to experimental measurements in a shock tube by Mao et al.[7] for fuel/“air” mixtures, equivalence ratios of 0.5, 1.0, and 1.5 and pressures of 10, 15, and 20 atm (Supporting Information, Fig. S1). The agreement between the simulations and experiments is similar to Fig. 3 below.

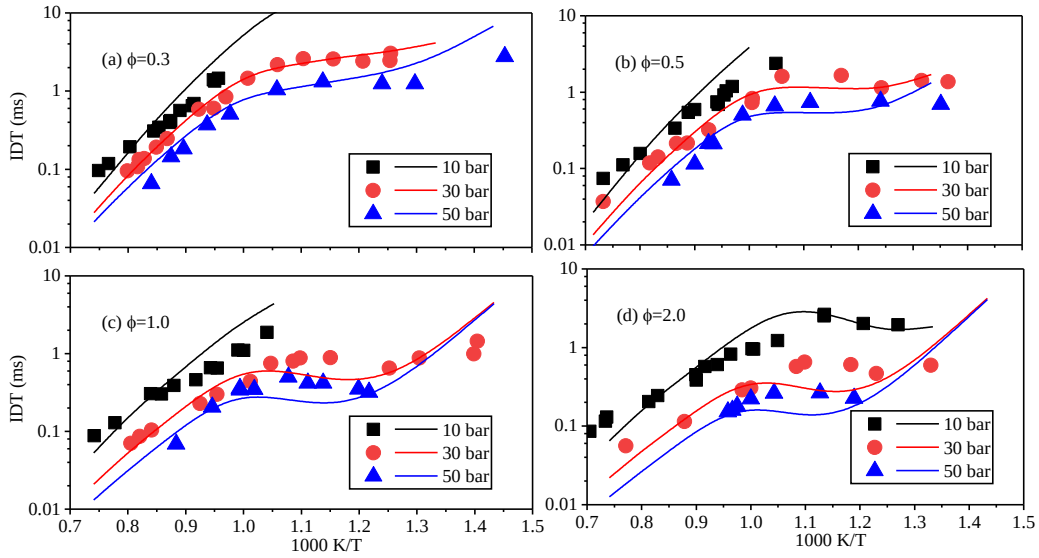

Figure 3. Experimental IDTs (symbols) for nBCH-"air" mixtures in the shock tube compared to those computed using the nBCH model (curves) for shock tube ignition for four equivalence ratios over a range of temperature and pressures of 10, 30, and 50 bar.

The experimentally measured total IDTs in the RCM are compared to the computed times in Fig. 4 for ϕ = 0.3, 0.5, 1.0 and 2.0 and pressures of 10 and 30 bar. In the calculations, volume histories for nonreactive mixtures were used to simulate the effect of compression and heat loss after the end of compression. Both the experiments and calculations showed a decrease in ignition delay time with increasing pressure from 10 to 30 bar and with increasing equivalence ratio from ϕ = 0.3 to 1.0. This is consistent with the ST data. NTC behavior was observed in the experimental ignition behavior at 10 atm at ϕ = 0.5 and 1.0. The simulated IDTs match the experimental results reasonably well. However, some difference can be seen in Fig 4(a) for 30 bar at the highest temperature, in Fig. 4(b) at 10 bar in the NTC region, and in Fig. 4(c, d) for 30 bar. The difference seen in Fig 4(a) for 30 bar at the highest temperature may be due to radical

pool build up in the simulation during the compression stroke because ignition is occurring so close to end of compression.

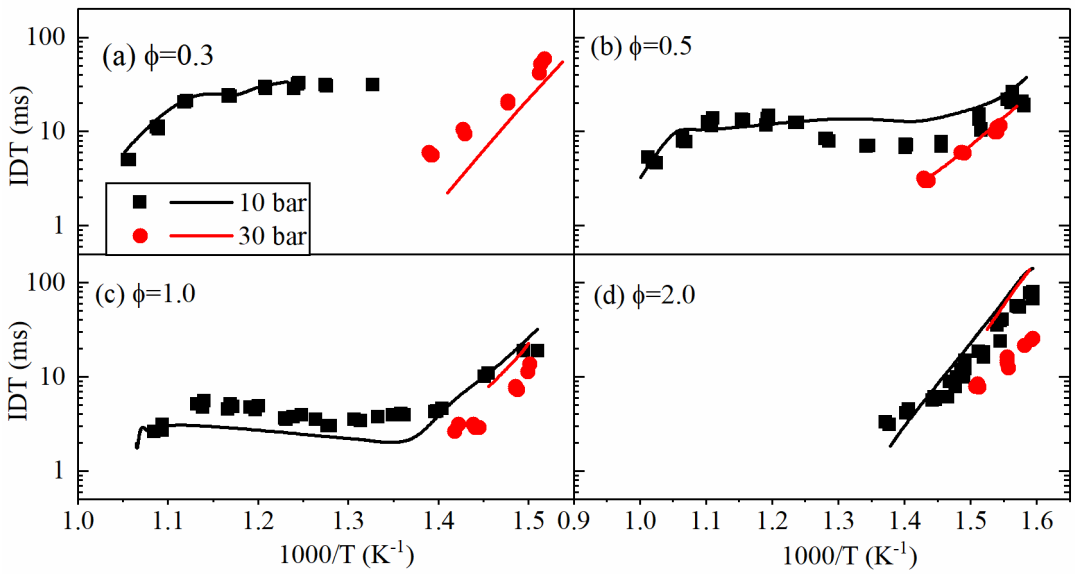

Figure 4. Experimental total IDTs (symbols) for nBCH-"air" mixtures in the RCM compared to those computed using the nBCH model (curves) for four equivalence ratios over a range of temperature and at pressures of 10 bar (black squares) and 30 bar (red circles).

Combined plots of the shock tube and RCM results are shown in Fig. 5 to compare the IDTs from the two experimental facilities and the associated simulated IDTs (curves). Overall, the agreement between the results of the simulations and the experiments is acceptable. In the transition region between experimental data from the ST and the RCM, the two sets of experimental data occasionally have some misalignment. The simulations which include facility effects in the RCM should account for these misalignments and this is the case for $\phi = 0.5$ and pressure 30 bar (Fig. 5b). However in the same figure at 10 bar, the simulations do not predict this misalignment and the simulations overpredict the IDTs in the lower temperature region of the ST experiments.

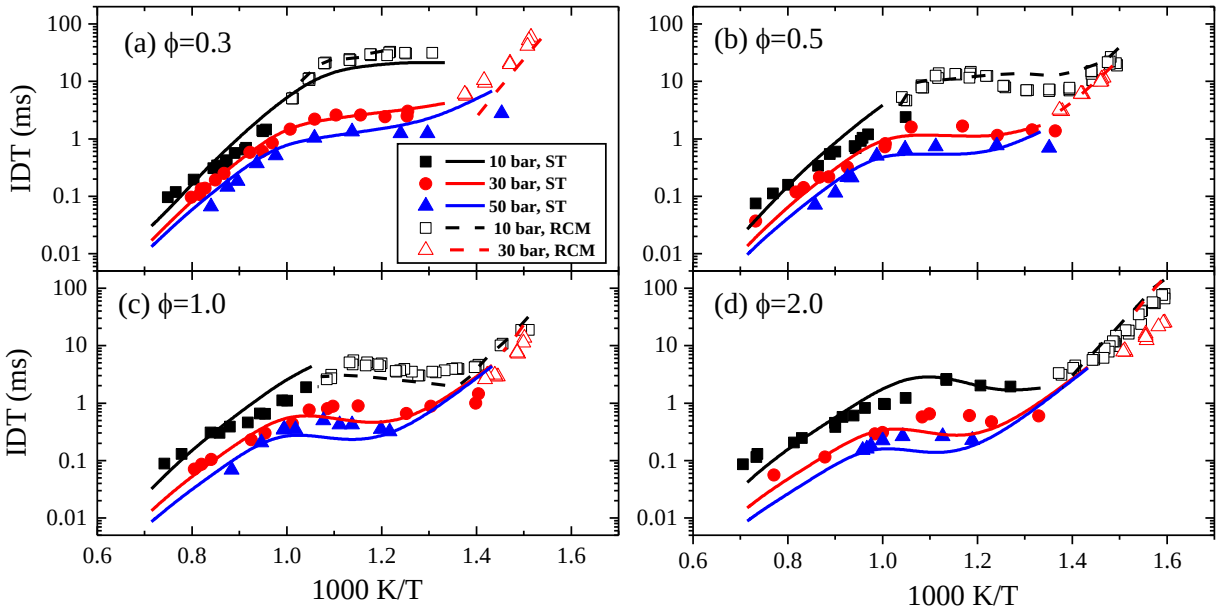

Figure 5: Combined results from the present work from the shock tube and RCM to compare the results between the two facilities. The solid symbols and the solid curves are the shock tube experiments and simulations. The open symbols and dashed curves are the RCM experiments and simulations. Results are given for four equivalence ratios of 0.3, 0.5, 1.0, and 2.0. The solid curves assumed constant volume combustion in the shock tube and the dashed curves used volume histories for nonreactive mixtures to simulate the effect of compression and heat loss after compression in the RCM.

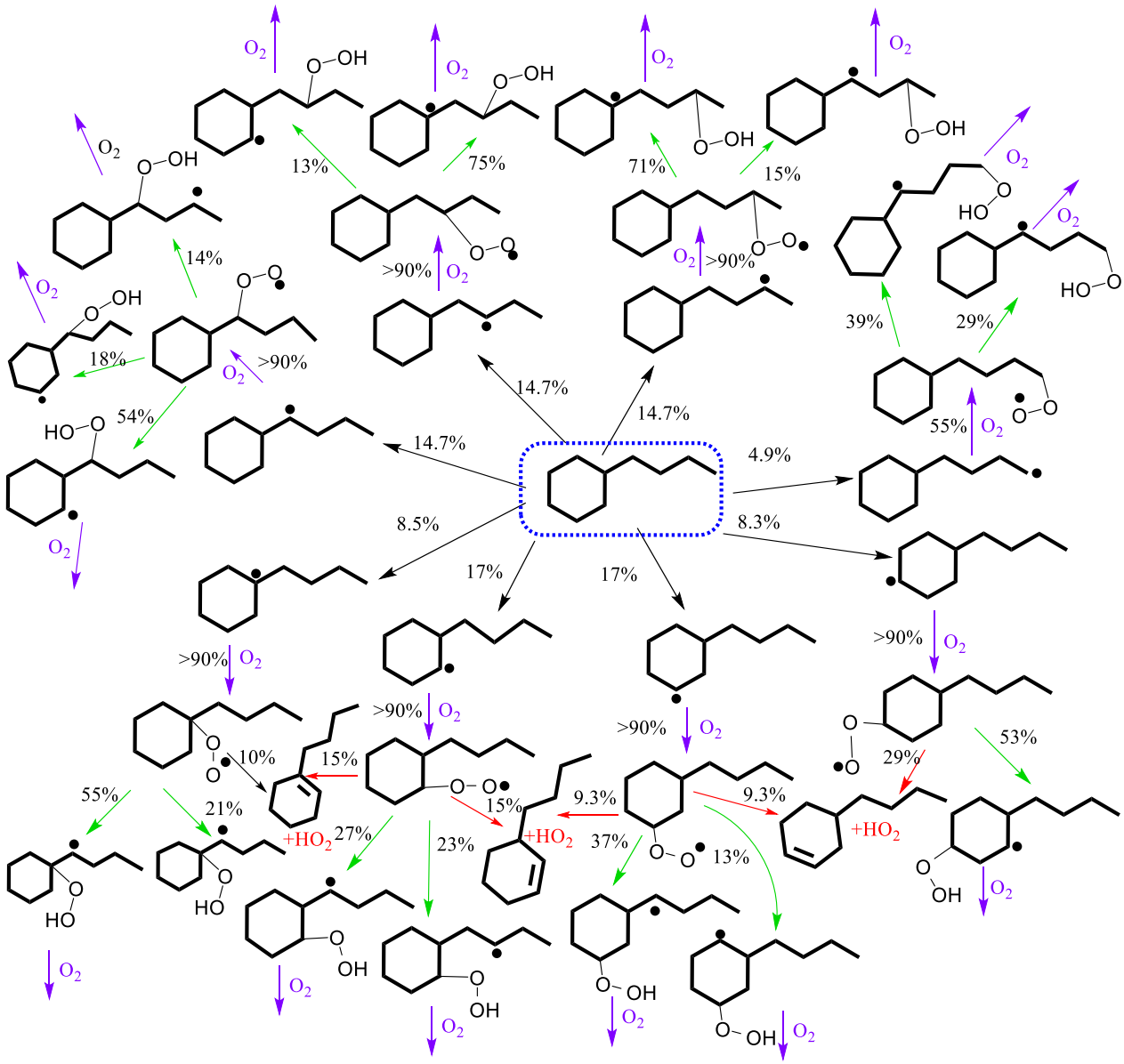

Figure 6. Flux analysis illustrating the important pathways in oxidation of nBCH. Analysis conducted using a constant volume simulation at 20% fuel conversion, starting with an initial pressure of 20 bar, an initial temperature of 775 K, and an equivalence ratio of 1.0.

A reaction path analysis was performed at conditions near the middle of the NTC region (775K) observed in the RCM experiments at 10 bar and ϕ = 1.0 (Fig. 6). The path analysis starts nBCH at the center of the figure giving the percentage of each radical formed and then expands outward with radical addition to O_2 and subsequent low temperature reactions. It can be seen

that the fuel radicals with radical sites on the 2 and 3 sites on the ring (see Fig. 2 for site nomenclature) are the most prevalent radicals because they can be formed by removing H atoms from either side of the ring. The next most prevalent radicals are those formed from secondary H-atom sites on the alkyl chain. In all cases, over 90% of the flux of these prevalent radicals proceeds through addition to O_2. For the A and B radicals on the alkyl chain (see Fig. 2 for nBCH labeling), their RO_2 radicals particularly lead to low temperature chain branching because they primarily undergo isomerization through a 6-member ring. QOOH formed from 6-membered rings favors low temperature chain branching leading to ketohydroperoxide + ȮH. This is because of the low ring-strain for 6-member rings that give a higher rate constant that exceeds the rate constant of the competing chain-propagating product path of cyclic ether + ȮH (not shown in Fig. 6 due to lack of space). QOOH formed from 6-membered rings can be seen in Fig. 6 as structures where the OOH group is γ to the radical site. RO_2 also reacts via 5-member ring transition-states to alkenes + HO_2, products that are shown in Fig. 6. For the A-radical leading to chain branching, ~54% of its associated RO_2 radical undergoes a 6-membered isomerization removing the H atom on the 2 position, giving the QOOH species named nBCH-AQ-2J (a key fuel species that appears in the sensitivity analysis discussed below). Also, ~75% of the RO_2 formed from the B-radical undergoes a 6-membered isomerization removing an H-atom from the 1 position (tertiary site) leading the chain branching. This reaction did not show up in the top 10 most sensitive reactions discussed below, probably because so much of this radical is already going to low temperature chain branching path (~75%) that further increasing its associated rate constants is not impactful on low temperature branching.

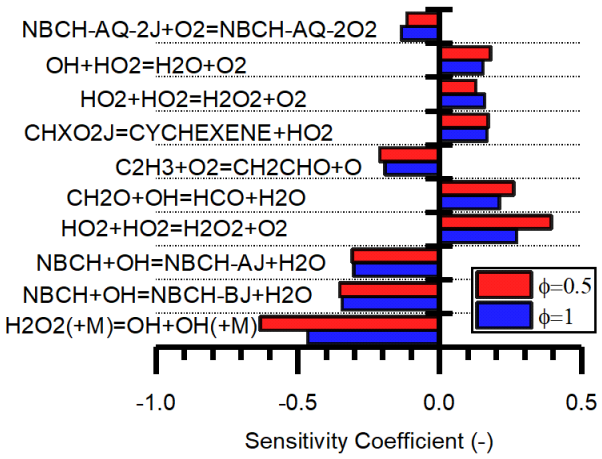

Figure 7: Reaction-rate constant sensitivity results for nBCH-"air" mixtures at 775K, 10 bar, and ϕ = 0.5 & 1.0.

To determine the controlling reactions in the NTC region in the RCM, a sensitivity analysis was performed on IDTs with respect to reaction rate constants at an initial pressure of 775K, an initial pressure of 10 bar and at ϕ = 0.5 & 1.0. Constant volume simulations were performed to compute the IDTs. The forward and reverse rate constants were multiplied by a factor of two and the sensitivity coefficients calculated using the log ratio of the perturbed and unperturbed IDTs. A negative sensitivity indicates a reaction promotes ignition and a positive sensitivity indicates a reaction inhibits ignition. The results are shown in Fig. 7 for the top 10 most sensitive reactions. The rate of the decomposition of H_2O_2 to form two ȮH radicals is the most sensitive reaction promoting ignition at both equivalence ratios. For inhibiting reactions, the self-reaction of HO_2 to form H_2O_2 and O_2 shows the highest sensitivity. Considering reactions involving the fuel, the reactions of nBCH with ȮH are the most sensitive, especially for abstraction on the A and B sites on the alkyl chain. These are same radical sites identified in the reaction path analysis as the ones most leading to low temperature chain branching. This observation is consistent with the result for the next most sensitive reaction NBCH-AQ-2J + O_2 <=> NBCH-AQ-2O_2 which is the addition

of QOOH to O2 and is on the path of low temperature chain branching for the A-radical. This reaction is shown as R1 in Fig. 8 and is followed by an 6-membered ring RO_2 isomerization that transfers an H atom on the A site to the peroxyl on the 2 site which leads to the rapid formation of an ȮH and a ketohydroperoxide (NBCH-A*O-2Q) (Fig. 8). The latter overall reaction step is represented by reaction R2. In methylcyclohexane (MCH), RO_2 isomerizations between sites that correspond to the aforementioned sites on nBCH have a low barrier and a higher rate constant compared to other RO_2 isomerizations in MCH low temperature chemistry[26, 41]. By analogy, the Weber et al.[26] isomerization rate constant for RO_2 in MCH was adapted for the RO_2 isomerization in nBCH involving an H-shift from site A to the peroxy group on site 2. An activation energy reduction of ~ 3 kcal was made for an H-abstraction on a secondary site in nBCH compared to a primary site in MCH, and the A-factor was adjusted for reaction degeneracy. Reaction R2 produces a ketohydroperoxide whose hydroperoxide group decomposes to another OH yielding chain branching. Because of the high sensitivity of IDTs to these low temperature reactions, quantum chemistry calculations are needed for nBCH to reduce the uncertainty in the rate constants for RO_2 isomerizations occurring between the ring and the alkyl chain.

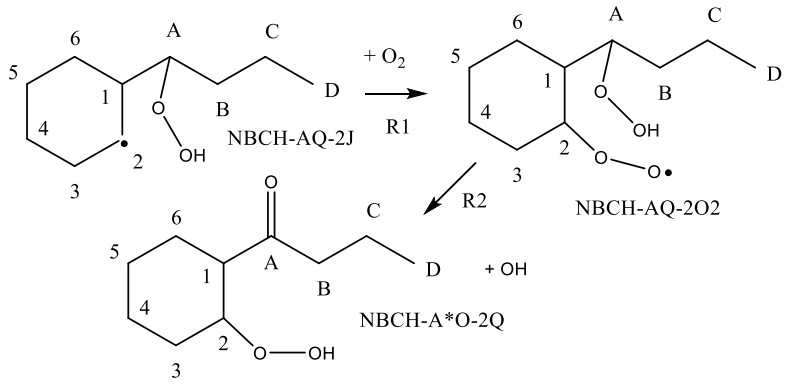

Figure 8. Most sensitive nBCH reaction involving low temperature chemistry is NBCH-AQ-2J + O_2 <=> NBCH-AQ-2O_2. It is followed by RO_2 isomerization involving site 2 and site A leading to an OH radical

and a ketohydroperoxide (NBCH-A*O-2Q). The hydroperoxide group on ketohydroperoxide decomposes to another OH, yielding chain branching.

Simulations using the nBCH model are also compared to literature results from a jet stirred reactor from Herbinet et al.[42]. A comparison of simulated and experimental results for species mole fractions for 500 – 1100K, 1.067 bar, and equivalence ratios of 0.25, 1.0 and 2.0 is shown in Fig. S2 (Supplementary Information). The agreement between the simulations and experiments of major species profiles (nBCH, O_2, CO, and CO_2) is good. For n-butylcyclohexene which are closely linked to the fuel chemistry is discussed above, the agreement is reasonable, but the agreement worsens for the lean case. For the other species, the most notable disagreement is for 1,3-butadiene which underpredicted by a factor of 3 for the lean and stoichiometric cases.

5. Conclusions

Ignition delay times for nBCH were measured in STs and an RCM over a range of temperatures from 630 to 1420 K, pressures of 10, 30, and 50 bar and equivalence ratios of 0.3, 0.5, 1.0, and 2.0. The experimental data set extended the upper limits of pressure in the literature from 20 bar to 50 bar in the shock tube and from 20 bar to 30 bar in the RCM. This extension of experimental data to higher pressures is important for validation of the model for diesel combustion applications. A detailed chemical kinetic model for nBCH was developed based on the previous ones developed for methylcyclohexane and cyclohexane. The kinetic model is validated over the wider pressure range provided by the new experimental data set. It was found that more recent $R\dot{O}_2$ isomerization rates based on *ab-initio* calculations provided better simulations of experimental data than previously used ones from Sarathy et al.[28] that were semi-empirically based. However, quantum chemistry calculations are still needed to compute

RO_2 isomerizations between the ring and the alkyl chain to further reduce the uncertainty in these rate constants. The newly developed kinetic model showed reasonable agreement with the new shock tube and RCM data. This model is now available for use as a surrogate-component model in a multicomponent diesel surrogate to help enable high-fidelity simulation of diesel fuels.

6. **References**

1. L. Turker, S. Varis, JP-900 Hydroperoxidation and Decomposition, Propellants Explosives Pyrotechnics 39 (2) (2014) 211-216.
2. W. S. Neill, W. L. Chippior, J. Cooley, M. Doma, C. Fairbridge, R. Falkiner, R. L. McCormick, K. Mitchell, *Emissions from Heavy-Duty Diesel Engine with EGR using Fuels Derived from Oil Sands and Conventional Crude*, SAE 2003-01-3144, Society of Automotive Engineers, 2003.
3. C. K. Westbrook, W. J. Pitz, M. Mehl, P. A. Glaude, O. Herbinet, S. Bax, F. Battin-Leclerc, O. Mathieu, E. L. Petersen, J. Bugler, H. J. Curran, Experimental and Kinetic Modeling Study of 2-Methyl-2-Butene: Allylic Hydrocarbon Kinetics, J. Phys. Chem. A 119 (28) (2015) 7462-7480.
4. C. S. McEnally, D. D. Das, L. D. Pfefferle, in: V1 ed.; Harvard Dataverse: 2017.
5. C. J. Mueller, W. J. Cannella, T. J. Bruno, B. Bunting, H. D. Dettman, J. A. Franz, M. L. Huber, M. Natarajan, W. J. Pitz, M. A. Ratcliff, K. Wright, Methodology for Formulating Diesel Surrogate Fuels with Accurate Compositional, Ignition-Quality, and Volatility Characteristics, Energy & Fuels 26 (6) (2012) 3284–3303.
6. C. J. Mueller, W. J. Cannella, J. T. Bays, T. J. Bruno, K. DeFabio, H. D. Dettman, R. M. Gieleciak, M. L. Huber, C.-B. Kweon, S. S. McConnell, W. J. Pitz, M. A. Ratcliff, Diesel Surrogate Fuels for Engine Testing and Chemical-Kinetic Modeling: Compositions and Properties, Energy & Fuels 30 (2) (2016) 1445-1461.
7. Y. Mao, S. Wang, Z. Wu, Y. Qiu, L. Yu, C. Ruan, F. Chen, L. Zhu, X. Lu, An experimental and kinetic modeling study of n-butylcyclohexane over low-to-high temperature ranges, Combust. Flame 206 (2019) 83-97.
8. Y. Mao, A. Li, L. Zhu, Z. Wu, L. Yu, S. Wang, M. Raza, X. Lu, A detailed chemical mechanism for low to high temperature oxidation of n-butylcyclohexane and its validation, Combust. Flame 210 (2019) 360-373.
9. R. H. Natelson, M. S. Kurman, N. P. Cernansky, D. L. Miller, Low temperature oxidation of n-butylcyclohexane, Combust. Flame 158 (12) (2011) 2325-2337.
10. Z. Hong, K.-Y. Lam, D. F. Davidson, R. K. Hanson, A comparative study of the oxidation characteristics of cyclohexane, methylcyclohexane, and n-butylcyclohexane at high temperatures, Combust. Flame 158 (8) (2011) 1456-1468.
11. B. Sirjean, E. Dames, D. A. Sheen, F. N. Egolfopoulos, H. Wang, D. F. Davidson, R. K. Hanson, H. Pitsch, C. T. Bowman, C. K. Law, W. Tsang, N. P. Cernansky, D. L. Miller, A. Violi, R. P. Lindstedt A high-temperature chemical kinetic model of n-alkane, cyclohexane, and methyl-, ethyl-, n-propyl and n-butylcyclohexaneoxidation at high temperatures, JetSurF version 1.1. http://melchior.usc.edu/JetSurF/JetSurF1.1 (September 15, 2010)
12. H. Wang, E. Dames, B. Sirjean, D. A. Sheen, R. Tangko, A. Violi, J. Y. W. Lai, F. N. Egolfopoulos, D. F. Davidson, R. K. Hanson, C. T. Bowman, C. K. Law, W. Tsang, N. P. Cernansky, D. L. Miller, R. P. Lindstedt A high-temperature chemical kinetic model of n-alkane (up to n-dodecane), cyclohexane, and methyl-, ethyl-, n-propyl and n-butyl-cyclohexane oxidation at high temperatures, JetSurF version 2.0, September 19, 2010. http://web.stanford.edu/group/haiwanglab/JetSurF/JetSurF2.0/ (1/30/2013)
13. M. A. Ali, V. T. Dillstrom, J. Y. W. Lai, A. Violi, Ab Initio Investigation of the Thermal Decomposition of n-Butylcyclohexane, J. Phys. Chem. A 118 (6) (2014) 1067-1076.
14. J. H. Kiefer, K. S. Gupte, L. B. Harding, S. J. Klippenstein, Shock Tube and Theory Investigation of Cyclohexane and 1-Hexene Decomposition, The Journal of Physical Chemistry A 113 (48) (2009) 13570-13583.
15. P. F. Flynn, R. P. Durrett, G. L. Hunter, A. O. z. Loye, O. C. Akinyemi, J. E. Dec, C. K. Westbrook, Diesel Combustion: An Integrated View Combining Laser Diagnostics, Chemical Kinetics, and Empirical Validation, Society of Automotive Engineers Transactions 108 (3) (1999) 587-600.

16. D. Darcy, C. J. Tobin, K. Yasunaga, J. M. Simmie, J. Wuermel, W. K. Metcalfe, T. Niass, S. S. Ahmed, C. K. Westbrook, H. J. Curran, A high pressure shock tube study of n-propylbenzene oxidation and its comparison with n-butylbenzene, Combust. Flame 159 (7) (2012) 2219-2232.
17. H. Nakamura, D. Darcy, M. Mehl, C. J. Tobin, W. K. Metcalfe, W. J. Pitz, C. K. Westbrook, H. J. Curran, An experimental and modeling study of shock tube and rapid compression machine ignition of n-butylbenzene/air mixtures, Combust. Flame 161 (1) (2014) 49-64.
18. C. Morley, *GasEq*, 0.76, http://www.gaseq.co.uk, 2004.
19. L. Brett. Re-commissioning of a rapid compression machine and computer modelling of hydrogen and methane autoignition. PhD Thesis, National University of Ireland, Galway, Galway, Ireland, 1999.
20. L. Brett, J. MacNamara, P. Musch, J. M. Simmie, Simulation of methane autoignition in a rapid compression machine with creviced pistons, Combust. Flame 124 (1-2) (2001) 326-329.
21. S. M. Gallagher, H. J. Curran, W. K. Metcalfe, D. Healy, J. M. Simmie, G. Bourque, A rapid compression machine study of the oxidation of propane in the negative temperature coefficient regime, Combust. Flame 153 (1-2) (2008) 316-333.
22. D. Healy, N. S. Donato, C. J. Aul, E. L. Petersen, C. M. Zinner, G. Bourque, H. J. Curran, n-Butane: Ignition delay measurements at high pressure and detailed chemical kinetic simulations, Combust. Flame 157 (8) (2010) 1526-1539.
23. J. Wurmel, J. M. Simmie, H. J. Curran, Studying the chemistry of HCCI in rapid compression machines, International Journal of Vehicle Design 44 (1-2) (2007) 84-106.
24. Y. Li, C.-W. Zhou, H. J. Curran, An extensive experimental and modeling study of 1-butene oxidation, Combust. Flame 181 (Supplement C) (2017) 198-213.
25. Y. Li, C.-W. Zhou, K. P. Somers, K. Zhang, H. J. Curran, The oxidation of 2-butene: A high pressure ignition delay, kinetic modeling study and reactivity comparison with isobutene and 1-butene, Proc. Combust. Inst. 36 (1) (2017) 403-411.
26. B. W. Weber, W. J. Pitz, M. Mehl, E. J. Silke, A. C. Davis, C.-J. Sung, Experiments and modeling of the autoignition of methylcyclohexane at high pressure, Combust. Flame 161 (8) (2014) 1972–1983.
27. R. Sivaramakrishnan, J. V. Michael, Shock tube measurements of high temperature rate constants for OH with cycloalkanes and methylcycloalkanes, Combust. Flame 156 (5) (2009) 1126-1134.
28. S. M. Sarathy, C. K. Westbrook, M. Mehl, W. J. Pitz, C. Togbé, P. Dagaut, H. Wang, M. A. Oehlschlaeger, U. Niemann, K. Seshadri, P. S. Veloo, C. Ji, F. N. Egolfopoulos, T. Lu, Comprehensive chemical kinetic modeling of the oxidation of 2-methylalkanes from C7 to C20, Combust. Flame 158 (12) (2011) 2338-2357.
29. W. S. McGivern, I. A. Awan, W. Tsang, J. A. Manion, Isomerization and decomposition reactions in the pyrolysis of branched hydrocarbons: 4-methyl-1-pentyl radical, J. Phys. Chem. A 112 (30) (2008) 6908-6917.
30. M. S. Stark, D. J. Waddington, Oxidation of Propene in the Gas-Phase, Int. J. Chem. Kinet. 27 (2) (1995) 123-151.
31. R. X. Fernandes, J. Zador, L. E. Jusinski, J. A. Miller, C. A. Taatjes, Formally direct pathways and low-temperature chain branching in hydrocarbon autoignition: the cyclohexyl + O2 reaction at high pressure, Physical Chemistry Chemical Physics 11 (9) (2009) 1320-1327.
32. A. Miyoshi, Molecular size dependent falloff rate constants for the recombination reactions of alkyl radicals with O2 and implications for simplified kinetics of alkylperoxy radicals, Int. J. Chem. Kinet. 44 (1) (2012) 59-74.
33. J. Bugler, K. P. Somers, E. J. Silke, H. J. Curran, Revisiting the Kinetics and Thermodynamics of the Low-Temperature Oxidation Pathways of Alkanes: A Case Study of the Three Pentane Isomers, J. Phys. Chem. A 119 (28) (2015) 7510-7527.
34. S. Sharma, S. Raman, W. H. Green, Intramolecular Hydrogen Migration in Alkylperoxy and Hydroperoxyalkylperoxy Radicals: Accurate Treatment of Hindered Rotors, The Journal of Physical Chemistry A 114 (18) (2010) 5689-5701.
35. N. J. Killingsworth, M. J. McNenly, R. A. Whitesides, S. W. Wagnon, Cloud based tool for analysis of chemical kinetic mechanisms, Combust. Flame 221 (2020) 170-179.
36. H. J. Curran, Rate constant estimation for C-1 to C-4 alkyl and alkoxyl radical decomposition, Int. J. Chem. Kinet. 38 (4) (2006) 250-275.
37. W. K. Metcalfe, S. M. Burke, S. S. Ahmed, H. J. Curran, A Hierarchical and Comparative Kinetic Modeling Study of C1 − C2 Hydrocarbon and Oxygenated Fuels, Int. J. Chem. Kinet. 45 (10) (2013) 638-675.
38. E. R. Ritter, J. W. Bozzelli, THERM - Thermodynamic Property Estimation for Gas-Phase Radicals and Molecules, Int. J. Chem. Kinet. 23 (9) (1991) 767-778.
39. J. W. Bozzelli, Group additivity data files, (2001).

40. M. F. Campbell, T. Parise, A. M. Tulgestke, R. M. Spearrin, D. F. Davidson, R. K. Hanson, Strategies for obtaining long constant-pressure test times in shock tubes, Shock Waves 25 (6) (2015) 651-665.
41. Y. Yang, A. L. Boehman, J. M. Simmie, Effects of molecular structure on oxidation reactivity of cyclic hydrocarbons: Experimental observations and conformational analysis, Combust. Flame 157 (12) (2010) 2369-2379.
42. O. Herbinet, B. Husson, H. Le Gall, F. Battin-Leclerc, Comparison study of the gas-phase oxidation of alkylbenzenes and alkylcyclohexanes, Chemical Engineering Science 131 (2015) 49-62.